Journal of Engineering Mathematics **31:** 81–98, 1997.

An efficient treatment of binary nonlinearities applied to elastic contact problems without friction

J.M. ALLWOOD*
Department of Mechanical Engineering, Imperial College of Science Medicine and Technology, Exhibition Road, London SW7 2BX, United Kingdom

R.E. STUBBS[1] and G.F. BRYANT[1]
[1]*Industrial Systems Group, IRC for Process Systems Engineering, Imperial College of Science Medicine and Technology, Exhibition Road, London SW7 2BY, United Kingdom*

Received 5 September 1995; accepted in revised form 22 March 1996

Abstract. The efficient solution of discrete models of contacting elastic bodies is investigated. At each discrete zone of the model the bodies are either in contact or not, so one of two possible linear system equations applies. The choice of equation in each zone is defined to be a binary nonlinearity. A weighting-function description of the elastic system is developed in which the binary nonlinearity is incorporated by use of partial Gauss-Jordan elimination of a model of full contact. This allows rapid solution to the contact problem. The solution scheme is shown to be stable as each iteration reduces the energy stored in the system. Worked examples are given. The work applies not only in contact mechanics, but also to other discrete models in which binary nonlinearities appear.

Key words: contact mechanics; binary nonlinearity; fast iterations; Gauss-Jordan elimination.

1. Introduction

A piecewise linear function with only two states is defined to have a binary nonlinearity. Examples of binary nonlinearities include uniaxial tensile stretching of an elastic perfectly-plastic wire, transmission of current through a diode, the relation of option to exercise price in a futures market and stick-slip friction. This paper investigates a further binary nonlinearity – the transmission of force across a mechanical contact interface.

The deformation of contacting linear elastic bodies is made nonlinear by uncertainty over the size and location of their mutual interface. The extent of contact between the bodies affects their shared stiffness and is dependent on the total force transmitted across the interface. This has given rise to extensive work defining mathematical expressions by which such behaviour can be described. The first work by Hertz [1], which gave an analytical solution for the elastic contact of quadratic surfaces, has been widely developed and an introduction to current understanding is given by Johnson [2]. Hills, Nowell and Sackfield [3] describe many contact geometries other than the simple parabola assumed by Hertz and explore issues related to tangential surface stresses due to friction.

Models of mechanical contact depend on knowledge of the elastic response of the approaching bodies. Typically, this is achieved through influence functions, i.e. the deformation response of the body to a point force. The most widely used of these is the 1892 solution of Flamant as treated by Timoshenko and Goodier [4. page 85]. This is for a point force acting on a semi-infinite solid and, while having the advantage of algebraic simplicity, is

* (to whom correspondence should be addressed)

limited by the need to define a radius at which deflections have reduced to zero. More accurate influence functions have been found for specific geometries, for instance Chiu et al [5] and Steven [6] have investigated the surface deformation of solid cylinders.

If two approaching bodies have a regular geometry, it may be possible to find analytic expressions for the extent of contact between them. However, analytic solutions for general geometries do not exist, so numerical methods must be used, in which the continuous fields of initial separation, contact force and displacement are sampled at fixed locations. Influence functions that describe deformation of the elastic bodies can be defined as vectors or matrices, thus allowing compact formulation, but uncertainty over the extent of contact leads to the use of iterative solutions. Chiu and Harnett [7] and Ahmadi et al [8] use an iterative scheme in which an initial estimate of the extent of contact is made and the model solved. The solution is then tested and the estimate of contact updated until the true solution is found but, as the whole model must be recalculated at each iterative step, this process is slow. For off-line studies this may not be important, but the work of this paper was motivated by a problem in the on-line control of metal rolling mills, where calculation speed is vital. Roll-bending jacks cause uncertainty over the extent of contact between rolls within a mill stack, so an iterative model of mill deformations must be used. However, improvement in mill-control algorithms required rapid model calculations, so a fast determination of the correct contact solution was required.

In an attempt to improve iteration procedures, Kalker and van Randen [9] have converted the binary nonlinearity of contact into a mathematical programming problem. Instead of solving directly for the contact force or distance in each zone of the discrete model, they find a solution by minimising the stored energy of the total contacting system. However, this does not remove the nonlinearity of the problem, but transforms it into a constraint on the solution space. Thus, the same difficulty of iteration remains and, in some cases, the non-negative constraints of the mathematical programming problem could be treated as another example of a binary nonlinearity to be addressed by the work of this paper. However, Kalker and van Randen's solution is more efficient than previous work, as the whole model need not be recalculated at each iterative step.

In this paper, a compact representation of contact uncertainty is presented. This is given either as a pair of matrix equations or as a single partitioned matrix problem. The partitioned form allows development of a solution method using partial Gauss-Jordan elimination in which, at each iterative step, only calculations related to zones of the discrete model whose contact status have changed are required. The iteration scheme so defined is shown to be stable.

2. Statement of the discrete contact problem

The linear elastic contact problem discussed in this paper is illustrated in Figure 1 with a deformable body approaching a rigid semi-infinite surface and just in contact when no force is applied. The vector **v** describes the distance between the undeformed body and the surface. A force F acts on the body, causing local deformation **u** at the mutual interface and overall approach D. The distributed force **f** (which by equilibrium integrates to F) acting at the interface is related to deformations **u** by the weighting function matrix $[W]$ such that

$$[W]\mathbf{f} = \mathbf{u}. \tag{1}$$

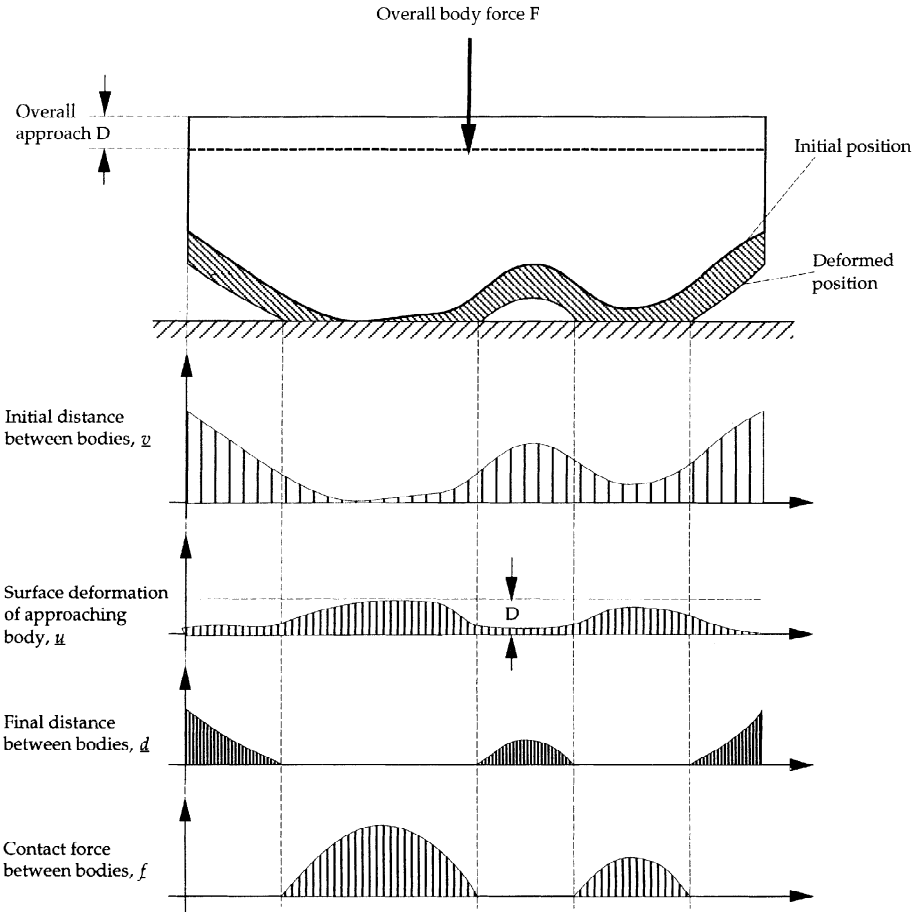

Figure 1. The general contact model – a contoured body approaches a rigid flat surface.

Allwood [10, p89] describes the uncertainty of contact at the interface of two bodies with a "binary-choice matrix" $[C]$. This is defined to have either ones or zeros on the leading diagonal (with a "one" representing contact) and zeros elsewhere. The forces and displacements at the contact interface must satisfy the conditions of Table 1.

Table 1. Mechanical conditions at a contact interface

	Interface force	Interface distance
Contact	Positive	0
Non-contact	0	Positive

From the geometry of Figure 1, the distance between the two bodies is calculated as

$$\mathbf{d} = \mathbf{v} + \mathbf{u} - D\boldsymbol{\theta}, \tag{2}$$

where $\boldsymbol{\theta}$ is a column vector of ones. Given a contact condition defined by $[C]$, the zero distance condition of Table 1 may thus be expressed as

$$[C]\mathbf{d} = [C]\mathbf{v} + [C][W]\mathbf{f} - D[C]\boldsymbol{\theta} = 0. \tag{3}$$

The zero-force condition at points of non-contact is given by

$$([I] - [C])\mathbf{f} = 0. \tag{4}$$

However, Equations (3) and (4) are not independent and can be summed, such that

$$([I] - [C] + [C][W])\mathbf{f} - D[C]\boldsymbol{\theta} = -[C]\mathbf{v}. \tag{5}$$

This has full rank and, given an estimated $[C]$ and the scalar condition of equilibrium, may be inverted to solve for the force distribution $\mathbf{f}$ and overall approach of the bodies, D. Equation (5) thus ensures that the two zero terms of Table 1 are satisfied. The choice of contact expressed by matrix $[C]$ is correct if all non-zero elements of the interface force and distance solution vectors are positive. These elements may also be selected by the binary choice matrix $[C]$ to form a test vector $\mathbf{V}$

$$\mathbf{V} = ([I] - [C])\mathbf{v} + (([I] - [C])[W] + [C])\mathbf{f} - D([I] - [C])\boldsymbol{\theta} \geq 0, \tag{6}$$

and will be positive only for the (unique) correct solution. Equations (5) and (6) thus give an efficient formulation for linear contact problems. However $[C]$ must be found iteratively and each step of the iteration will be slow if the matrices of Equation (5) are large.

3. Expression in partitioned matrix form

Equation (5), while compact, disguises some of the structure of this problem. The expression may, without loss of information, be transformed by use of a permutation matrix which re-orders the sampling points used to describe the discrete model. The chosen permutation (described by matrix $[T]$ with inverse $[T]'$) collects all rows corresponding to points not in contact as the first part of each vector. Developing Equation (5),

$$\begin{aligned}
&[T]([I] - [C] + [C][W])\mathbf{f} - D[T][C]\boldsymbol{\theta} = -[T][C]\mathbf{v},\\
&[T]([I] - [C] + [C][W])[T']\mathbf{f} - D[T][C][T']\boldsymbol{\theta} = -[T][C][T'][T]\mathbf{v},\\
&([I] - [T][C][T'] + [T][C][T'][T][W][T'])[T]\mathbf{f} - D[T][C][T'][T]\boldsymbol{\theta} = -[T][C][T'][T]\mathbf{v},\\
&([I] - [\tilde{C}] + [\tilde{C}][\tilde{W}])\tilde{\mathbf{f}} - D[\tilde{C}]\tilde{\boldsymbol{\theta}} = -[\tilde{C}]\tilde{\mathbf{v}},
\end{aligned} \tag{7}$$

in which a tilda indicates that the order of the original discretisation has been altered. The last line of Equation (7) has the same structure as Equation (5) so the permutation matrix does not affect the shape of the equation. The matrix $[\tilde{C}]$ will now have zeros along the first part of the leading diagonal and ones thereafter. Let the weighting-function matrix $[\tilde{W}]$ (which, by the reciprocal theorem, is symmetric,) be partitioned as

$$[\tilde{W}] = \begin{bmatrix} \tilde{W}_{1,1} & \tilde{W}_{1,2} \\ \tilde{W}'_{1,2} & \tilde{W}_{2,2} \end{bmatrix}, \tag{8}$$

in which the location of the partition coincides with the change from non-contact to contact in $[\tilde{C}]$. Equation (5) may now be written in combination with the force equilibrium condition as

$$\begin{bmatrix} [I] & 0 & 0 \\ 0 & \tilde{W}_{2,2} & \boldsymbol{\theta} \\ 0 & \boldsymbol{\theta}' & 0 \end{bmatrix} \begin{Bmatrix} \mathbf{f}_1 \\ \mathbf{f}_2 \\ -D \end{Bmatrix} = \begin{Bmatrix} 0 \\ -\mathbf{v}_2 \\ F \end{Bmatrix}. \tag{9}$$

In this expression, the force and undeformed distance vectors have been split into two components. Those indicated by the subscript 1 represent model zones not in contact, while those with subscript 2 give locations in contact. The first row of Equation (9) ensures that force outside the contact region is zero. The second row ensures zero penetration within the contact region and the last row defines force equilibrium. The unknown distance of approach between the bodies is given as negative, so that all elements of the left-side matrix are non-negative. Symmetry is maintained. The test vector **V** defined by (6) may also be given in partitioned matrix form as

$$\mathbf{V} = \begin{Bmatrix} \tilde{\mathbf{d}}_1 \\ \tilde{\mathbf{f}}_2 \\ -D \end{Bmatrix} = \begin{bmatrix} \tilde{W}_{1,1} & \tilde{W}_{1,2} & \boldsymbol{\theta}_1 \\ 0 & I & 0 \\ 0 & 0 & 1 \end{bmatrix} \begin{Bmatrix} \tilde{\mathbf{f}}_1 \\ \tilde{\mathbf{f}}_2 \\ -D \end{Bmatrix} + \begin{Bmatrix} \tilde{\mathbf{v}}_1 \\ 0 \\ 0 \end{Bmatrix}, \tag{10}$$

in which the third row has been maintained to keep the matrix square. However, this may be expanded by the solution of (9). To simplify model notation, the last row and column of the partitions in (9) and (10) (the force equilibrium condition) will be incorporated into the equations for the contact region, giving

$$\begin{bmatrix} I & 0 \\ 0 & \tilde{L}_{2,2} \end{bmatrix} \left\{ \begin{Bmatrix} \tilde{\mathbf{f}}_1 \\ \tilde{\mathbf{f}}_2 \end{Bmatrix} \right\} = \left\{ \begin{Bmatrix} 0 \\ -\tilde{\mathbf{v}}_2 \end{Bmatrix} \right\} \tag{11}$$

and

$$\left\{ \begin{Bmatrix} \tilde{\mathbf{d}}_1 \\ \tilde{\mathbf{f}}_2 \end{Bmatrix} \right\} = \begin{bmatrix} \tilde{L}_{1,1} & \tilde{L}_{1,2} \\ 0 & I \end{bmatrix} \left\{ \begin{Bmatrix} \tilde{\mathbf{f}}_1 \\ \tilde{\mathbf{f}}_2 \end{Bmatrix} \right\} - \left\{ \begin{Bmatrix} \tilde{\mathbf{v}}_1 \\ 0 \end{Bmatrix} \right\}. \tag{12}$$

If the solution of (11) is now substituted in (12), then the test vector **V** is found by

$$\begin{aligned} \left\{ \begin{Bmatrix} \tilde{\mathbf{d}}_1 \\ \tilde{\mathbf{f}}_2 \end{Bmatrix} \right\} &= \begin{bmatrix} \tilde{L}_{1,1} & \tilde{L}_{1,2} \\ 0 & I \end{bmatrix} \begin{bmatrix} I & 0 \\ 0 & \tilde{L}_{2,2}^{-1} \end{bmatrix} \left\{ \begin{Bmatrix} 0 \\ \tilde{\mathbf{v}}_2 \end{Bmatrix} \right\} - \left\{ \begin{Bmatrix} -\tilde{\mathbf{v}}_1 \\ 0 \end{Bmatrix} \right\} \\ &= \begin{bmatrix} -I & \tilde{L}_{1,2}\tilde{L}_{2,2}^{-1} \\ 0 & \tilde{L}_{2,2}^{-1} \end{bmatrix} \left\{ \begin{Bmatrix} -\tilde{\mathbf{v}}_1 \\ -\tilde{\mathbf{v}}_2 \end{Bmatrix} \right\}. \end{aligned} \tag{13}$$

Use of the permutation matrix $[T]$ has thus allowed transformation of the contact model into a simple partitioned matrix form. The contact problem will be solved once the binary choice matrix $[C]$ and hence the permutation matrix $[T]$ have been found such that all elements of the vectors $\tilde{\mathbf{d}}_1$ and $\tilde{\mathbf{f}}_2$ of Equation (13) are positive.

4. Rapid recursive solution of the contact model

Non-negative solution of (13) is required to find the correct contact conditions. The solution must be iterative, should be rapid at each step and must be stable. This section demonstrates a rapid solution technique and its stability is investigated in section 5.

4.1. SOLUTION WITH PERMUTED PARTITIONED MATRICES

Assume that the approaching bodies are in full contact. The forces between them are found from (8) and (9) as the solution of

$$\begin{bmatrix} \tilde{W}_{1,1} & \tilde{W}_{1,2} & \boldsymbol{\theta}_1 \\ \tilde{W}'_{1,2} & \tilde{W}_{2,2} & \boldsymbol{\theta}_2 \\ \boldsymbol{\theta}'_1 & \boldsymbol{\theta}'_2 & 0 \end{bmatrix} \begin{Bmatrix} \tilde{\mathbf{f}}_1 \\ \tilde{\mathbf{f}}_2 \\ -D \end{Bmatrix} = \begin{Bmatrix} -\tilde{\mathbf{v}}_1 \\ -\tilde{\mathbf{v}}_2 \\ F \end{Bmatrix}$$

$$\text{or} \quad \begin{bmatrix} \tilde{L}_{1,1} & \tilde{L}_{1,2} \\ \tilde{L}'_{1,2} & \tilde{L}_{2,2} \end{bmatrix} \begin{Bmatrix} \tilde{\mathbf{f}}_1 \\ \begin{Bmatrix} \tilde{\mathbf{f}}_2 \\ -D \end{Bmatrix} \end{Bmatrix} = \begin{Bmatrix} -\tilde{\mathbf{v}}_1 \\ \begin{Bmatrix} -\tilde{\mathbf{v}}_2 \\ F \end{Bmatrix} \end{Bmatrix}. \tag{14}$$

solving the second form of (14) by Gauss-Jordan elimination, after one step, we find

$$\begin{bmatrix} \tilde{L}_{1,1} - \tilde{L}_{1,2}\tilde{L}_{2,2}^{-1}\tilde{L}'_{1,2} & 0 \\ \tilde{L}_{2,2}^{-1}\tilde{L}'_{1,2} & I \end{bmatrix} \begin{Bmatrix} \tilde{\mathbf{f}}_1 \\ \begin{Bmatrix} \tilde{\mathbf{f}}_2 \\ -D \end{Bmatrix} \end{Bmatrix} = \begin{bmatrix} I & -\tilde{L}_{1,2}\tilde{L}_{2,2}^{-1} \\ 0 & \tilde{L}_{2,2}^{-1} \end{bmatrix} \begin{Bmatrix} \tilde{\mathbf{v}}_1 \\ \begin{Bmatrix} -\tilde{\mathbf{v}}_2 \\ F \end{Bmatrix} \end{Bmatrix}. \tag{15}$$

Although this is part of the solution of the full contact situation, the right side of (15) is, apart from the sign of the top row, identical to the right side of (13) which describes partial contact. This convenient feature of Gauss-Jordan elimination, described in the simpler case of a beam on multiple supports by Gantmacher [11, p28], allows development of a fast solution to the entire problem.

Equation (13) was developed with the assumption that the points described by vectors $\mathbf{f}_1$ and $\mathbf{d}_1$ were not in contact, while those represented by $\mathbf{f}_2$ and $\mathbf{d}_2$ were. In this case all elements of $\mathbf{f}_1$ will be zero, so the bottom row of (15) is identical to the force solution given by (9). The top row of the right-hand side of (15) gives (negatively) the distance between the two bodies, $\mathbf{d}_1$. Thus, (15) calculates the two non-zero components of Table 1, while all elements of the other two components have been forced to zero.

Interpretation of Equation (15) depends on an assumption of contact conditions, represented by the division of the unknown forces into $\mathbf{f}_1$ and $\mathbf{f}_2$. Given this assumption and the zero elements of Table 1, Equation (15) retains redundant information – the right column of the left side matrix and the left column of the right side matrix, which will always comprise zeros and the identity in the manner shown. All of the information in the two matrices of Equation (15) may thus be held in one "storage" matrix, as

$$[\tilde{S}] = \begin{bmatrix} \tilde{L}_{1,1} - \tilde{L}_{1,2}\tilde{L}_{2,2}^{-1}\tilde{L}'_{1,2} & -\tilde{L}_{1,2}\tilde{L}_{2,2}^{-1} \\ \tilde{L}_{2,2}^{-1}\tilde{L}'_{1,2} & \tilde{L}_{2,2}^{-1} \end{bmatrix}. \tag{16}$$

The advantage of this storage matrix is that it allows an efficient continuation of the solution. Equation (15) assumes certain contact conditions, which will be verified by the left side vector of Equation (13). However, if part of the estimated contact region has been specified incorrectly, so that the lower part of $\mathbf{d}_1$ is negative, Equation (15) may be expanded as

$$\begin{bmatrix} \tilde{L}_{1,1}^{(i)} - \tilde{L}_{1,3}^{(i)}\tilde{L}_{3,3}^{(i)^{-1}}\tilde{L}_{1,3}^{(i)'} & \tilde{L}_{1,2}^{(i)} - \tilde{L}_{1,3}^{(i)'}\tilde{L}_{3,3}^{(i)^{-1}}\tilde{L}_{2,3}^{(i)'} & 0 \\ \tilde{L}_{1,2}^{(i)} - \tilde{L}_{2,3}^{(i)}\tilde{L}_{3,3}^{(i)^{-1}}\tilde{X}'_{1,3} & \tilde{L}_{2,2}^{(i)} - \tilde{L}_{2,3}^{(i)}\tilde{L}_{3,3}^{(i)^{-1}}\tilde{L}_{2,3}^{(i)} & 0 \\ \tilde{L}_{3,3}^{(i)^{-1}}\tilde{L}_{1,3}^{(i)} & \tilde{L}_{3,3}^{(i)^{-1}}\tilde{L}_{2,3}^{(i)} & I \end{bmatrix} \begin{Bmatrix} \tilde{\mathbf{f}}_1^+ \\ \tilde{\mathbf{f}}_1^- \\ \begin{Bmatrix} \tilde{\mathbf{f}}_2 \\ -D \end{Bmatrix} \end{Bmatrix} = \begin{bmatrix} I & 0 & -\tilde{L}_{1,3}^{(i)}\tilde{L}_{3,3}^{(i)^{-1}} \\ 0 & I & -\tilde{L}_{2,3}^{(i)}\tilde{L}_{3,3}^{(i)^{-1}} \\ 0 & 0 & \tilde{L}_{3,3}^{(i)^{-1}} \end{bmatrix} \begin{Bmatrix} -\tilde{\mathbf{v}}_1^+ \\ -\tilde{\mathbf{v}}_1^- \\ \begin{Bmatrix} -\tilde{\mathbf{v}}_2 \\ F \end{Bmatrix} \end{Bmatrix}$$

$$\text{or} \quad \begin{bmatrix} \tilde{L}_{1,1}^{(i+1)} & \tilde{L}_{1,2}^{(i+1)} & 0 \\ \tilde{L}_{2,1}^{(i+1)} & \tilde{L}_{2,2}^{(i+1)} & 0 \\ \tilde{L}_{3,1}^{(i+1)} & \tilde{L}_{3,2}^{(i+1)} & I \end{bmatrix} \begin{Bmatrix} \tilde{\mathbf{f}}_1^+ \\ \tilde{\mathbf{f}}_1^- \\ \begin{Bmatrix} \tilde{\mathbf{f}}_2 \\ -D \end{Bmatrix} \end{Bmatrix} = \begin{bmatrix} I & 0 & \tilde{R}_{1,3}^{(i+1)} \\ 0 & I & \tilde{R}_{2,3}^{(i+1)} \\ 0 & 0 & \tilde{R}_{3,3}^{(i+1)} \end{bmatrix} \begin{Bmatrix} -\tilde{\mathbf{v}}_1^+ \\ -\tilde{\mathbf{v}}_1^- \\ \begin{Bmatrix} -\tilde{\mathbf{v}}_2 \\ F \end{Bmatrix} \end{Bmatrix}. \tag{17}$$

The partitioned notation here has been extended to three blocks and the superscripted number refers to the current stage of the Gauss-Jordan elimination process. The error in the test vector of (13) implies that the elimination of (15) must be continued. This is achieved by pre-multiplying both sides of (17) by the matrix,

$$[\tilde{M}] = \begin{bmatrix} I & -\tilde{L}_{1,2}^{(i+1)} \tilde{L}_{2,2}^{(i+1)^{-1}} & 0 \\ 0 & \tilde{L}_{2,2}^{(i+1)^{-1}} & 0 \\ 0 & -\tilde{L}_{3,2}^{(i+1)} \tilde{L}_{2,2}^{(i+1)^{-1}} & I \end{bmatrix} \tag{18}$$

to obtain

$$\begin{bmatrix} \tilde{L}_{1,1}^{(i+1)} - \tilde{L}_{1,2}^{(i+1)} \tilde{L}_{2,2}^{(i+1)} \tilde{L}_{2,1}^{(i+1)} & 0 & 0 \\ \tilde{L}_{2,2}^{(i+1)^{-1}} \tilde{L}_{2,1}^{(i+1)} & I & 0 \\ \tilde{L}_{3,1}^{(i+1)} - \tilde{L}_{2,3}^{(i+1)} \tilde{L}_{2,2}^{(i+1)^{-1}} \tilde{L}_{2,1}^{(i+1)} & 0 & I \end{bmatrix} \begin{Bmatrix} \tilde{\mathbf{f}}_1^+ \\ \tilde{\mathbf{f}}_1^- \\ \begin{Bmatrix} \tilde{\mathbf{f}}_2 \\ -D \end{Bmatrix} \end{Bmatrix}$$

$$= \begin{bmatrix} I & -\tilde{L}_{1,2}^{(i+1)} \tilde{L}_{2,2}^{(i+1)^{-1}} & \tilde{R}_{1,3}^{(i+1)} - \tilde{L}_{1,2}^{(i+1)} \tilde{L}_{2,2}^{(i+1)^{-1}} \tilde{R}_{2,3}^{(i+1)} \\ 0 & \tilde{L}_{2,2}^{(i+1)^{-1}} & \tilde{L}_{2,2}^{(i+1)^{-1}} \tilde{R}_{2,3}^{(i+1)} \\ 0 & -\tilde{L}_{2,3}^{(i+1)} \tilde{L}_{2,2}^{(i+1)^{-1}} & \tilde{R}_{3,3}^{(i+1)} - \tilde{L}_{2,3}^{(i+1)} \tilde{L}_{2,2}^{(i+1)^{-1}} \tilde{R}_{2,3}^{(i+1)} \end{bmatrix} \begin{Bmatrix} \tilde{\mathbf{v}}_1^+ \\ \tilde{\mathbf{v}}_1^- \\ \begin{Bmatrix} \tilde{\mathbf{v}}_2 \\ -F \end{Bmatrix} \end{Bmatrix},$$

$$\begin{bmatrix} \tilde{L}_{1,1}^{(i+2)} & 0 & 0 \\ \tilde{L}_{2,1}^{(i+2)} & I & 0 \\ \tilde{L}_{3,1}^{(i+2)} & 0 & I \end{bmatrix} \begin{Bmatrix} \tilde{\mathbf{f}}_1^+ \\ \tilde{\mathbf{f}}_1^- \\ \begin{Bmatrix} \tilde{\mathbf{f}}_2 \\ -D \end{Bmatrix} \end{Bmatrix} = \begin{bmatrix} I & \tilde{R}_{1,2}^{(i+2)} & \tilde{R}_{1,3}^{(i+2)} \\ 0 & \tilde{R}_{2,2}^{(i+2)} & \tilde{R}_{2,3}^{(i+2)} \\ 0 & \tilde{R}_{3,2}^{(i+2)} & \tilde{R}_{3,3}^{(i+2)} \end{bmatrix} \begin{Bmatrix} \tilde{\mathbf{v}}_1^+ \\ \tilde{\mathbf{v}}_1^- \\ \begin{Bmatrix} \tilde{\mathbf{v}}_2 \\ F \end{Bmatrix} \end{Bmatrix}. \tag{19}$$

Had the error in contact conditions been that less contact was required rather than more, the expression of (19) should be pre-multiplied by the (updated) inverse of (18),

$$[\tilde{M}] = \begin{bmatrix} I & \tilde{L}_{1,2}^{(i+1)} & 0 \\ 0 & \tilde{L}_{2,2}^{(i+1)} & 0 \\ 0 & \tilde{L}_{3,2}^{(i+1)} & I \end{bmatrix} = \begin{bmatrix} I & -\tilde{R}_{1,2}^{(i+2)} \tilde{R}_{2,2}^{(i+2)^{-1}} & 0 \\ 0 & \tilde{R}_{2,2}^{(i+2)^{-1}} & 0 \\ 0 & -\tilde{R}_{2,3}^{(i+2)} \tilde{R}_{2,2}^{(i+2)^{-1}} & I \end{bmatrix}, \tag{20}$$

which causes a return to (17). The similarity of expressions (20) and (18) shows that the matrix $[M]$ is formed from $[S]$ by identical means, regardless of whether contact is to be increased or decreased. After i stages of the iteration, consider $[S]$ as partitioned into three

rows and columns, of which the central row and column represent mis-specified points of contact. Then, regardless of the current contact status of the mis-specified points, the required pre-multiplication matrix is found as

$$[\tilde{M}] = \begin{bmatrix} I & -\tilde{S}^{(i)}_{1,2}\tilde{S}^{(i)^{-1}}_{2,2} & 0 \\ 0 & \tilde{S}^{(i)^{-1}}_{2,2} & 0 \\ 0 & -\tilde{S}^{(i)}_{3,2}\tilde{S}^{(i)^{-1}}_{2,2} & I \end{bmatrix} \tag{21}$$

The next iteration of $[S]$ – which holds the information in both left and right sides of (19) – can be found by three stages of overwriting:

$$\begin{aligned}
\begin{bmatrix} \tilde{S}^{(i)}_{1,1} & \tilde{S}^{(i)}_{1,2} & \tilde{S}^{(i)}_{1,3} \\ \tilde{S}^{(i)}_{2,1} & \tilde{S}^{(i)}_{2,2} & \tilde{S}^{(i)}_{2,3} \\ \tilde{S}^{(i)}_{3,1} & \tilde{S}^{(i)}_{3,2} & \tilde{S}^{(i)}_{3,3} \end{bmatrix} &\leftarrow \begin{bmatrix} \tilde{S}^{(i)}_{1,1} & -\tilde{S}^{(i)}_{1,2}\tilde{S}^{(i)^{-1}}_{2,2} & \tilde{S}^{(i)}_{1,3} \\ \tilde{S}^{(i)}_{2,1} & \tilde{S}^{(i)^{-1}}_{2,2} & \tilde{S}^{(i)}_{2,3} \\ \tilde{S}^{(i)}_{3,1} & -\tilde{S}^{(i)}_{3,2}\tilde{S}^{(i)^{-1}}_{2,2} & \tilde{S}^{(i)}_{3,3} \end{bmatrix} \\
&\leftarrow \begin{bmatrix} \tilde{S}^{(i)}_{1,1} - \tilde{S}^{(i)}_{1,2}\tilde{S}^{(i)^{-1}}_{2,2}\tilde{S}^{(i)}_{2,1} & -\tilde{S}^{(i)}_{1,2}\tilde{S}^{(i)^{-1}}_{2,2} & \tilde{S}^{(i)}_{1,3} - \tilde{S}^{(i)}_{1,2}\tilde{S}^{(i)^{-1}}_{2,2}\tilde{S}^{(i)}_{2,3} \\ \tilde{S}^{(i)}_{2,1} & \tilde{S}^{(i)^{-1}}_{2,2} & \tilde{S}^{(i)}_{2,3} \\ \tilde{S}^{(i)}_{3,1} - \tilde{S}^{(i)}_{3,2}\tilde{S}^{(i)^{-1}}_{2,2}\tilde{S}^{(i)}_{2,1} & -\tilde{S}^{(i)}_{3,2}\tilde{S}^{(i)^{-1}}_{2,2} & \tilde{S}^{(i)}_{3,3} - \tilde{S}^{(i)}_{3,2}\tilde{S}^{(i)^{-1}}_{2,2}\tilde{S}^{(i)}_{2,3} \end{bmatrix} \\
&\leftarrow \begin{bmatrix} \tilde{S}^{(i)}_{1,1} - \tilde{S}^{(i)}_{1,2}\tilde{S}^{(i)^{-1}}_{2,2}\tilde{S}^{(i)}_{2,1} & -\tilde{S}^{(i)}_{1,2}\tilde{S}^{(i)^{-1}}_{2,2} & \tilde{S}^{(i)}_{1,3} - \tilde{S}^{(i)}_{1,2}\tilde{S}^{(i)^{-1}}_{2,2}\tilde{S}^{(i)}_{2,3} \\ \tilde{S}^{(i)^{-1}}_{2,2}\tilde{S}^{(i)}_{2,1} & \tilde{S}^{(i)^{-1}}_{2,2} & \tilde{S}^{(i)^{-1}}_{2,2}\tilde{S}^{(i)}_{2,3} \\ \tilde{S}^{(i)}_{3,1} - \tilde{S}^{(i)}_{3,2}\tilde{S}^{(i)^{-1}}_{2,2}\tilde{S}^{(i)}_{2,1} & -\tilde{S}^{(i)}_{3,2}\tilde{S}^{(i)^{-1}}_{2,2} & \tilde{S}^{(i)}_{3,3} - \tilde{S}^{(i)}_{3,2}\tilde{S}^{(i)^{-1}}_{2,2}\tilde{S}^{(i)}_{2,3} \end{bmatrix} \\
&= \begin{bmatrix} \tilde{S}^{(i+1)}_{1,1} & \tilde{S}^{(i+1)}_{1,2} & \tilde{S}^{(i+1)}_{1,3} \\ \tilde{S}^{(i+1)}_{2,1} & \tilde{S}^{(i+1)}_{2,2} & \tilde{S}^{(i+1)}_{2,3} \\ \tilde{S}^{(i+1)}_{3,1} & \tilde{S}^{(i+1)}_{3,2} & \tilde{S}^{(i+1)}_{3,3} \end{bmatrix}
\end{aligned} \tag{22}$$

(The backward arrow "←" in (22) represents an overwriting operation.) Thus Equation (22) gives a compact description of the evolution of a recursive solution to the contact problem. Thus far the formulation requires an update to the permutation matrix $[T]$ at each iterative step, to ensure that all incorrectly specified contact points accumulate in a band in the middle of the unknown force vector. The contact status of each mis-specified point must be reversed, by use of a matrix corresponding to (18). The storage matrix is then updated by (22) and the record of contact status of each point amended. The process is repeated until the test vector **V** is all non-negative. The process of updating the permutation matrix is time consuming. However, the transformation $[T]$ and the use of tilda notation have become redundant because the overwriting operation is identical, regardless of whether it is to increase or reduce the region of contact. The next section describes a direct solution process.

4.2. SOLUTION WITHOUT PERMUTATION

Define a vector $\boldsymbol{\alpha}^{(i)}$ which contains the indices of all elements of the discretisation assumed to be in contact after the i^{th} iteration. Let $\boldsymbol{\alpha}_c^{(i)}$ be the indices of all other points. The vector of contact force is now $\mathbf{f}(\boldsymbol{\alpha}^{(i)})$, while every element of $\mathbf{f}(\boldsymbol{\alpha}_c^{(i)})$ will be zero. For convenience in notation, $\boldsymbol{\alpha}$ is assumed to extend by one point to include the force equilibrium equation, so the last element of $\boldsymbol{\alpha}$ must always give the index $(N+1)$ where N is the number of zones in the model. Let the vector $\boldsymbol{\beta}$ contain the indices of all elements that fail the conditions of Table 1 and $\boldsymbol{\beta}^c$ contain the indices of those that pass. The vectors $\boldsymbol{\alpha}$ and $\boldsymbol{\beta}$ and their complements may be used to describe the overwriting scheme of (22) without the need for tilda notation:

Initialise: Prepare the storage matrix $[S]$ which for zero contact corresponds to the left side of (14). Set $\boldsymbol{\alpha}$ to zeros and initialise $\boldsymbol{\beta}$ to a first estimate of the contact region (including the index $(N+1)$). An efficient first estimate is found by comparison of the initial distance between the bodies with their deformation under the action of an even distribution of the force F. Thus $\boldsymbol{\beta}$ is initialised to all points for which $\mathbf{v} < \frac{F}{N}[W]\boldsymbol{\theta}$

Step 1: Update the storage matrix according to $\boldsymbol{\beta}$. The three stages of updating in partitioned form given as (22) can be represented as four stages using $\boldsymbol{\beta}$:

$$\begin{aligned}
&1)\ S^{(i+1)}(\boldsymbol{\beta},\boldsymbol{\beta}) \ \leftarrow S^{(i)}(\boldsymbol{\beta},\boldsymbol{\beta})^{-1},\\
&2)\ S^{(i+1)}(\boldsymbol{\beta}^c,\boldsymbol{\beta}) \leftarrow -S^{(i)}(\boldsymbol{\beta}^c,\boldsymbol{\beta})S^{(i+1)}(\boldsymbol{\beta},\boldsymbol{\beta}),\\
&3)\ S^{(i+1)}(\boldsymbol{\beta}^c,\boldsymbol{\beta}^c)\leftarrow S^{(i)}(\boldsymbol{\beta}^c,\boldsymbol{\beta}^c) + S^{(i+1)}(\boldsymbol{\beta}^c,\boldsymbol{\beta})S^{(i)}(\boldsymbol{\beta},\boldsymbol{\beta}^c),\\
&4)\ S^{(i+1)}(\boldsymbol{\beta},\boldsymbol{\beta}^c) \leftarrow S^{(i+1)}(\boldsymbol{\beta},\boldsymbol{\beta})S^{(i)}(\boldsymbol{\beta},\boldsymbol{\beta}^c).
\end{aligned} \tag{23}$$

The superscripts indicating iteration number have been included to emphasise the utility of overwriting: updating the matrix requires no extra storage.
Update the current contact status $\boldsymbol{\alpha}$ by

$$\boldsymbol{\alpha}^{(i+1)} = (\boldsymbol{\alpha}^{(i)} \cap \boldsymbol{\beta}^c) \cup (\boldsymbol{\alpha}_c^{(i)} \cap \boldsymbol{\beta}) \tag{24}$$

Reset $\boldsymbol{\beta}$ to zeros.

Step 2: Form the test vectors:

$$\begin{aligned}
\mathbf{d}(\boldsymbol{\alpha}^c) \ &= \ -S(\boldsymbol{\alpha}^c,\boldsymbol{\alpha})\mathbf{R}(\boldsymbol{\alpha}) - \mathbf{R}(\boldsymbol{\alpha}^c),\\
\left\{\begin{matrix}\mathbf{f}(\boldsymbol{\alpha})\\ -D\end{matrix}\right\} \ &= \ S(\boldsymbol{\alpha},\boldsymbol{\alpha})\mathbf{R}(\boldsymbol{\alpha}),
\end{aligned} \tag{25}$$

in which $\mathbf{R}$ is the right side vector of (14). Obviously, all elements of the two complements $\mathbf{d}(\boldsymbol{\alpha})$ and $\mathbf{f}(\boldsymbol{\alpha}^c)$ are zeros.

Step 3: If any elements of either of the test vectors of (25) are negative, place their indices in $\boldsymbol{\beta}$ and return to step 1. Otherwise the solution is complete.

This scheme is computationally efficient. Row and column selection is simple, and only the first step of (23) requires inversion, the others being multiplication or addition operations. The size of the matrix to be inverted is equal to the number of points currently mis-specified, so becomes smaller as the solution is approached. The model of section 2 required re-inversion of the full matrix at each iterative step. The recursive model proposed here requires a series of smaller inversions, such that the worst step that could occur in this scheme is equivalent to one stage of the iteration in section 2. The remaining requirement to prove the technique's applicability is to investigate its stability.

5. Investigation of solution stability

The mechanical system of Figure 1 is conservative and the equilibrium solution to the contact problem will be that with minimum stored energy. The stored energy of the system, U, is equal to the work done by external forces. With the assumption of adiabatic compression it may be defined as

$$U = F \times D. \tag{26}$$

The stability of the scheme of section 4 is investigated through the two situations of Figure 2. In Figure 2a, the estimated region of contact was too great and the interfacial force negative in region 2. In Figure 2b, the estimated contact region was too small and the interfacial distance negative in region 2. By use of the permutation matrix $[T]$, all iterations of the model may be shown to conform to one of these two situations and if the response to each can be shown to reduce the stored energy of the system, the solution will be stable.

Consider the situation of Figure 2a. Given the monotonic and strongly convex surface of the body, contact will be made or lost in strict order through the discretisation scheme, so tilda notation is unnecessary in this discussion. The first iteration (denoted by superscript (1)) assumes full contact in regions 1 and 2. From Equation (14)) this is described by

$$\begin{bmatrix} W_{1,1} & W_{1,2} & \boldsymbol{\theta}_1 \\ W'_{1,2} & W_{2,2} & \boldsymbol{\theta}_2 \\ \boldsymbol{\theta}'_1 & \boldsymbol{\theta}'_2 & 0 \end{bmatrix} \begin{Bmatrix} \mathbf{f}_1^{(1)} \\ \mathbf{f}_2^{(1)} \\ -D^{(1)} \end{Bmatrix} = \begin{Bmatrix} -\mathbf{v}_1 \\ -\mathbf{v}_2 \\ F \end{Bmatrix}. \tag{27}$$

The test vector $\mathbf{V}$ for this full contact situation comprises the two force vectors, but, as illustrated in Figure 2a, $\mathbf{f}_1^{(1)} \geq 0$, while $\mathbf{f}_2^{(1)} < 0$. The stored energy of the system is

$$U^{(1)} = F \times D^{(1)}. \tag{28}$$

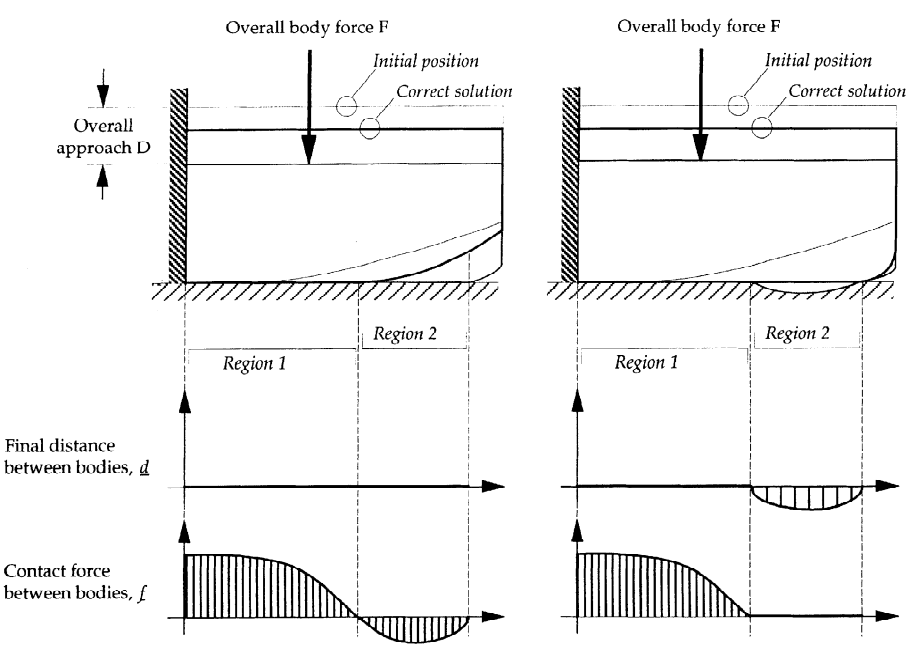

Figure 2. a) Over-specification of contact area. b) Under-specification of contact area.

As the scalar input force remains constant, stability is achieved if $D^{(2)} < D^{(1)}$. The iterative scheme proposed in the previous section requires that points in region 2 be released from contact in the second iteration, so

$$\begin{bmatrix} W_{1,1} & 0 & \boldsymbol{\theta}_1 \\ 0 & I & 0 \\ \boldsymbol{\theta}_1' & 0 & 0 \end{bmatrix} \begin{Bmatrix} \mathbf{f}_1^{(2)} \\ \mathbf{f}_2^{(2)} \\ -D^{(2)} \end{Bmatrix} = \begin{Bmatrix} -\mathbf{v}_1 \\ 0 \\ F \end{Bmatrix}, \tag{29}$$

which drives the second region of force to zero, $\mathbf{f}_2^{(2)} = 0$. The first row of Equation (27) is rearranged and subtracted from the first row of Equation (29) to give

$$(D^{(1)} - D^{(2)})\boldsymbol{\theta}_1 = [W_{11} \quad W_{12}] \begin{Bmatrix} \mathbf{f}_1^{(1)} - f_1^{(2)} \\ \mathbf{f}_2^{(1)} \end{Bmatrix} = [W_{11} \quad W_{12}] \begin{Bmatrix} \mathbf{f}_1^{(*)} \\ \mathbf{f}_2^{(1)} \end{Bmatrix}, \tag{30}$$

in which the vector, $\mathbf{f}_1^{(*)}$ is obviously defined. The force vector on the right side of (30) must sum to zero, as both solutions (27) and (29) are in equilibrium with the same input force F. The term $\mathbf{f}_2^{(1)}$ is all negative, so $\mathbf{f}_1^{(*)}$ has a positive sum. Development of (30) gives

$$\boldsymbol{\theta}_1' W_{11}^{-1} \boldsymbol{\theta}_1 (D^{(1)} - D^{(2)}) = \boldsymbol{\theta}_1' \mathbf{f}_1^{(*)} + \boldsymbol{\theta}_1' W_{11}^{-1} W_{12} \mathbf{f}_2^{(1)}, \tag{31}$$

in which the left-side scalar $\boldsymbol{\theta}_1' W_{11}^{-1} \boldsymbol{\theta}_1$ is positive, as W_{11} is symmetric positive definite (the physical system is conservative.) Consider the last component of the right side of (31). Let

$$\mathbf{y} = W_1^{-1} 1 W_{12} \mathbf{f}_2^{(1)}, \text{ or } W_{11}\mathbf{y} = W_{12}\mathbf{f}_2^{(1)}. \tag{32}$$

The physical effect of $\mathbf{y}$ and $\mathbf{f}_2^{(1)}$ in Figure 2a is that $\mathbf{y}$ is the force acting in region 1 required to cause the same displacement in region 1 as that caused by the given force $\mathbf{f}_2^{(1)}$ acting on region 2. As the influence of a point force decays with distance from its point of application (and hence the size of elements in the matrix W decrease monotonically away from the leading diagonal) it is certain that

$$\boldsymbol{\theta}_1' \cdot \mathbf{y} < \boldsymbol{\theta}_2' \cdot \mathbf{f}_2^{(1)}. \tag{33}$$

Rearranging (31), using (33) and the fact that the right vector of (30) sums to zero, we obtain

$$\begin{aligned} D^{(1)} - D^{(2)} &= \frac{1}{\boldsymbol{\theta}_1' W_{11}^{-1} \boldsymbol{\theta}_1} (\boldsymbol{\theta}_1' \mathbf{f}_1^{(*)} + \boldsymbol{\theta}_1' W_{11}^{-1} W_{12} \mathbf{f}_2^{(1)}) \\ &> \frac{1}{\boldsymbol{\theta}_1' W_{11}^{-1} \boldsymbol{\theta}_1} (\boldsymbol{\theta}_1' \mathbf{f}_1^{(*)} + \boldsymbol{\theta}_2' \mathbf{f}_2^{(1)}) > 0, \end{aligned} \tag{34}$$

which, from (28), is the result required to prove the stability of the iteration scheme in the case illustrated in Figure 2a.

A related argument holds in Figure 2b. Let us assume that the region in which contact is mis-specified is a single zone, so only one row of the system matrix is updated. Thus one point of region 2 is now assumed to be not in contact, so the system equation is

$$\begin{bmatrix} W_{1,1} & 0 & \boldsymbol{\theta}_1 \\ 0 & 1 & 0 \\ \boldsymbol{\theta}_1' & 0 & 0 \end{bmatrix} \begin{Bmatrix} \mathbf{f}_1^{(1)} \\ f_2^{(1)} \\ -D^{(1)} \end{Bmatrix} = \begin{Bmatrix} -\mathbf{v}_1 \\ 0 \\ F \end{Bmatrix}. \tag{35}$$

The contact condition used to define Equation (35) does not solve the model, as there is overlap between the surfaces in region 2 – the distance between them is negative:

$$d_2^{(1)} = v_2 + \mathbf{W}'_{1,2}\mathbf{f}_1^{(1)} - D^{(1)} < 0. \tag{36}$$

The next iteration re-defines the point in region 2 as being in contact, and stability will again be proven if the stored energy of the system is reduced. Let the updated force distribution $\mathbf{f}_2$, comprise the solution to Equation (35) plus a zero sum component $\mathbf{f}^*$,

$$\begin{Bmatrix} \mathbf{f}_1^{(2)} \\ f_2^{(2)} \end{Bmatrix} = \begin{Bmatrix} \mathbf{f}_1^{(1)} \\ 0 \end{Bmatrix} + \begin{Bmatrix} \mathbf{f}_1^{(*)} \\ f_2^{(*)} \end{Bmatrix}. \tag{37}$$

After the change of contact conditions, Equation (35) becomes

$$\begin{bmatrix} W_{1,1} & \mathbf{W}_{1,2} & \boldsymbol{\theta}_1 \\ \mathbf{W}'_{1,2} & W_{2,2} & 1 \\ \boldsymbol{\theta}'_1 & 1 & 0 \end{bmatrix} \begin{Bmatrix} \mathbf{f}_1^{(1)} + \mathbf{f}_1^{(*)} \\ f_2^{(*)} \\ -D^{(2)} \end{Bmatrix} = \begin{Bmatrix} -\mathbf{v}_1 \\ -\mathbf{v}_2 \\ F \end{Bmatrix}. \tag{38}$$

The second row of this expression substituted in (36) yields the inequality

$$(D^{(1)} - D^{(2)}) + \mathbf{W}'_{1,2}\mathbf{f}_1^{(*)} + W_{2,2}f_2^{(*)} > 0. \tag{39}$$

Equation (39) may be combined with the difference between the first rows of Equations (35) and (38) and the zero sum condition for $\mathbf{f}^*$ to give

$$\begin{bmatrix} W_{1,1} & \mathbf{W}_{1,2} & \boldsymbol{\theta}_1 \\ \mathbf{W}'_{1,2} & W_{2,2} & 1 \\ \boldsymbol{\theta}'_1 & 1 & 0 \end{bmatrix} \begin{Bmatrix} \mathbf{f}_1^{(*)} \\ f_2^{(*)} \\ D^{(1)} - D^{(2)} \end{Bmatrix} = \begin{Bmatrix} 0 \\ \varepsilon \\ 0 \end{Bmatrix}. \tag{40}$$

in which ε is equal to the left side of Equation (39) and is positive. (Equation (40) describes a system in which two bodies are held in contact by adhesion at their interface, without the application of an external force, and with an initial geometry that would fit perfectly, except at the point indicated by ε.) Equation (40) may be rewritten with only two partitions as

$$\begin{bmatrix} W & \boldsymbol{\theta} \\ \boldsymbol{\theta}' & 0 \end{bmatrix} \begin{Bmatrix} \mathbf{f}^* \\ D^{(1)} - D^{(2)} \end{Bmatrix} = \begin{Bmatrix} \mathbf{e} \\ 0 \end{Bmatrix}, \tag{41}$$

in which $\mathbf{e}$ is a vector of zeros except for the last element which contains ε. After partial Gaussian elimination, Equation (41) becomes

$$\begin{bmatrix} I & W^{-1}\boldsymbol{\theta} \\ 0 & -\boldsymbol{\theta}'W^{-1}\boldsymbol{\theta} \end{bmatrix} \begin{Bmatrix} \mathbf{f}^* \\ D^{(1)} - D^{(2)} \end{Bmatrix} = \begin{Bmatrix} W^{-1}\mathbf{e} \\ -\boldsymbol{\theta}'W^{-1}\mathbf{e} \end{Bmatrix}, \tag{42}$$

and hence

$$D^{(1)} - D^{(2)} = \frac{\boldsymbol{\theta}'W^{-1}\mathbf{e}}{\boldsymbol{\theta}'W^{-1}\boldsymbol{\theta}}. \tag{43}$$

The denominator of this equation is again positive as the matrix $[W]$ is positive definite. The numerator must also be positive as it calculates the total force required to produce a positive displacement. Therefore

$$D^{(1)} - D^{(2)} > 0, \tag{44}$$

which by Equation (28) proves a reduction in stored energy as a result of the iterative response to under-specification of contact by one point. Under-specification by more than one point will be stable by the obvious extension of the above proof.

Thus the iterative scheme has been shown to be stable under both types of error in specifying contact. Any estimate of the contact region may be used for the first iteration and all subsequent estimates are found by reversing the contact state of any erroneous points in the previous iteration. This guarantees convergence on the correct solution.

6. Non-recursive solution with near full contact

The solution method of section 4 is recursive – the storage matrix is overwritten at each iteration. This is the most general solution to the contact problem, but an alternative method can be used if a large contact region is expected and the solution matrix is not required. Comparison of the solution method in section 4 with the description of the Sherman-Morrison formula given in Hager [12] suggests that a faster approach may be possible when only a few points of the solution are not in contact. This approach firstly requires calculation of the solution to the full contact problem, then at each iteration modifies it according to the region in which contact is lost. Define $\hat{\mathbf{V}}$ as the solution vector with full contact, given in two-block partitioned form with tilda notation as

$$\hat{\mathbf{V}} = \begin{Bmatrix} \tilde{\mathbf{f}}_1 \\ \left\{ \begin{array}{c} \tilde{f}_2 \end{array} \right\} \\ -D \end{Bmatrix} = \begin{bmatrix} \tilde{R}_{1,1} & \tilde{R}_{1,2} \\ \tilde{R}_{2,1} & \tilde{R}_{2,2} \end{bmatrix} \begin{Bmatrix} -\tilde{\mathbf{v}}_1 \\ \left\{ \begin{array}{c} -\tilde{\mathbf{v}}_2 \end{array} \right\} \\ F \end{Bmatrix}. \tag{45}$$

As this is a full contact solution, all elements of $\hat{\mathbf{V}}$ refer to force, not distance. If the elements of $\tilde{\mathbf{f}}_1$ are negative and those of $\tilde{\mathbf{f}}_2$ are positive, the next iteration in the solution involves a pre-multiplication of both sides of (41) by a matrix $[\tilde{M}]$ derived from (20) as

$$[\tilde{M}] = \begin{bmatrix} I & -\tilde{R}_{1,1}^{-1}\tilde{R}_{1,2} \\ 0 & \tilde{R}_{2,2} - \tilde{R}_{2,1}\tilde{R}_{1,1}^{-1}\tilde{R}_{1,2} \end{bmatrix}. \tag{46}$$

With sign changes as before, we find the updated estimate of the test vector $\mathbf{V}$ as

$$\mathbf{V} = \begin{bmatrix} I & -\tilde{R}_{1,1}^{-1}\tilde{R}_{1,2} \\ 0 & \tilde{R}_{2,2} - \tilde{R}_{2,1}\tilde{R}_{1,1}^{-1}\tilde{R}_{1,2} \end{bmatrix} \begin{bmatrix} \tilde{R}_{1,1} & \tilde{R}_{1,2} \\ \tilde{R}_{2,1} & \tilde{R}_{2,2} \end{bmatrix} \begin{Bmatrix} -\tilde{\mathbf{v}}_1 \\ \left\{ \begin{array}{c} -\tilde{\mathbf{v}}_2 \end{array} \right\} \\ F \end{Bmatrix} = \begin{bmatrix} -\tilde{R}_{1,1}^{-1} & 0 \\ -\tilde{R}_{2,1}\tilde{R}_{1,1}^{-1} & I \end{bmatrix} \hat{\mathbf{V}}. \tag{47}$$

Provided the number of points of contact lost is small, so that $\tilde{R}_{1,1}^{-1}$ is calculated quickly, this potentially offers a faster solution to that of section 4. At each iteration, the estimated contact region is updated and the test vector $\mathbf{V}$ recalculated from (47). As before, tilda notation is

only used for convenience and the operation of (47) can be achieved with the vector $\boldsymbol{\alpha}$ used to select rows and columns of the stored matrix, such that,

$$\mathbf{V} = \begin{bmatrix} -S(\alpha^c,\alpha^c)^{-1} & 0 \\ -S(\alpha,\alpha^c)S(\alpha^c,\alpha^c)^{-1} & I \end{bmatrix} \begin{Bmatrix} \hat{\mathbf{V}}(\alpha^c) \\ \hat{\mathbf{V}}(\alpha) \end{Bmatrix} = \begin{Bmatrix} -S(\alpha^c,\alpha^c)^{-1}\hat{\mathbf{V}}(\alpha^c) \\ \hat{\mathbf{V}}(\alpha) - S(\alpha,\alpha^c)S(\alpha^c,\alpha^c)^{-1}\hat{\mathbf{V}}(\alpha^c) \end{Bmatrix}. \tag{48}$$

Solution of (48) is rapid if the two bodies are largely in contact, but as $\tilde{R}_{1,1}^{-1}$ must be found at each iteration, calculation time will progressively increase as contact loss increases.

7. Example solutions

A simple example of the proposed solution methods is given to illustrate the speed of the technique. A contoured solid body is brought towards a rigid half space, under the action of three different scalar forces in turn. The influence function is that given by Johnson [2] for the surface normal deflection to a uniform pressure P acting over a region of length $2a$:

$$u_z(x) = \frac{(1-\nu^2)}{\pi E} P \left\{ (x+a)\ln\left(\frac{x+a}{a}\right)^2 - (x-a)\ln\left(\frac{x-a}{a}\right)^2 \right\} + k \tag{49}$$

(The constant k is unknown but does not affect the example given, where only relative deformation is important). Model dimensions have been chosen to illustrate three different contact regions from the same physical system. The model is solved by the original $[C]$ matrix technique of section 2, the recursive storage-matrix technique of section 4 and the non-recursive vectorised solution of section 6. The initial distance between bodies has been chosen to allow three extreme contact situations: nearly full contact; mixed regions of contact and non-contact; very narrow band of contact. the process follows identical iterations regardless of solution method and these are illustrated for the three different overall loads in Figure 3. (The plots for iteration 0 indicate the distance between the bodies at first contact, before force is applied.) The iterations are initialised according to the suggestion of section 4. Clearly this is successful in Figures 3a and 3c. In Figure 3b the final contact configuration is more complex and the process requires more iterations.

The methods are compared, for a model discretised over 300 points, in Table 2. The method of section 2 is slow as the full matrix must be inverted at each iteration. With the recursive method of section 4, each successive iteration is quicker, as speed depends on change in contact conditions from the previous iteration. The non-recursive method of section 6 requires a first slow iteration in which the full matrix is inverted. Subsequent iteration times are proportional to the total number of non-contacting points and in the first case of Table 2 with nearly full contact, are the quickest achieved by any method, but are slow in the third case where most of the body is not in contact.

8. Discussion and extensions

The work of this paper has derived and demonstrated a rapid technique for the general description of binary nonlinearities which has been applied to elastic contact problems without friction. The technique has been shown to be stable. The examples given above used a Flamant influence function, but the technique may be used with any other influence function. The example was also one dimensional, but a two or three-dimensional contact could be treated

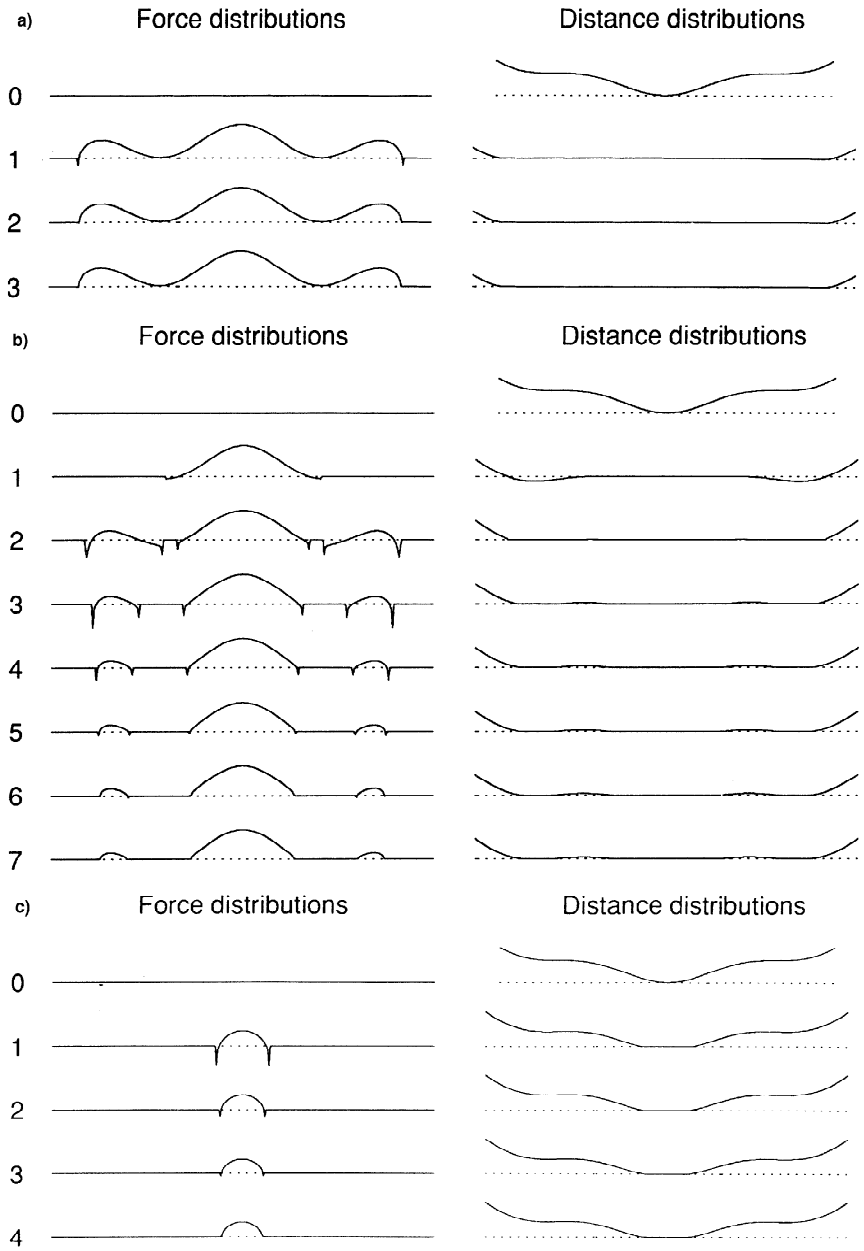

Figure 3. Force and displacement distributions during iterative solution of test problem with a) $F = 300$, b) $F = 150$, c) $F = 30$.

similarly. Further to this, the same method could be used to describe more complex surface deformation, including surface traction due to friction.

Implementation of the technique may lead to matrix conditioning problems, as the test vector **V** contains elements of force and distance. The problem may be overcome by rescaling the units. The solution given here has also not exploited the inevitable symmetry of the weighting-function matrix. This is principally an implementation issue and is well explored elsewhere in the literature, but will yield useful increases in calculation speed.

Table 2. Timing comparisons of three solution methods to the elastic contact problem.

Total applied force		Section 2 method	Section 4 method	Section 6 method
F = 300	*Iteration 1*	61.88	14.49	16.49
	2	60.60	1.38	0.12
	3	60.58	0.66	0.13
		= 183.06	**= 16.53**	**= 16.74**
F = 150	*Iteration 1*	64.18	7.54	19.74
	2	64.18	8.82	0.32
	3	63.79	3.59	1.43
	4	61.27	1.48	2.20
	5	61.78	1.00	2.73
	6	61.38	0.75	3.04
	7	61.44	0.67	3.30
		= 434.59	**= 23.85**	**= 32.76**
F = 30	*Iteration 1*	62.67	2.51	26.82
	2	62.02	0.70	11.20
	3	62.03	0.53	11.45
	4	62.24	0.54	11.65
		= 248.96	**= 4.28**	**= 61.11**

The proof of iterative stability in section 5 assumed that the influence functions forming the columns of $[W]$ were monotonically decreasing from the leading diagonal. This will be true for any expression describing surface deflections only but does not hold, for instance, in the contact of two simply supported beams whose greatest deflection will be central, regardless of where the force acts. This work was motivated by the need to describe the deflection of metal rolling mills with accuracy and speed. The deflection of rolls in the stack comprises components related to both beam bending of the roll axis and local surface flattening. In that case, local flattening under the point of application of the force is greater than maximum beam bending and the solution remains stable. Further work on stability of the iterations would be useful in defining more general limits on solution convergence.

The examples of solution shown in Figure 3 indicate the stability of the method as predicted, but also show that the iterative scheme of reversing the contact status of currently mis-specified points may be conservative. Analysis of stored energy after each iteration would allow more rapid convergence without significantly more calculation complexity in each step. Such an approach could be investigated in the context of the work by Kalker and van Randen [9], although their use of a general quadratic programming algorithm is likely to be less efficient than the scheme proposed here which takes advantage of the physical structure of the problem to work directly towards the one feasible point of the solution.

Subsequent to his earlier paper, Kalker [13, ch 4] gives more details of his iterative scheme. It has many similarities to the approach given in section 2 here: an estimate of the contact region is made; a model based on the equality constraints of table one is solved; the non-negative requirements for penetration and interfacial force are tested and adjusted by the same “toggling” used here; the process is repeated until all elements of the solution vectors are non-negative. Kalker solves a more general problem than this paper, including interfacial shear forces and stick-slip friction. He also poses the problem in two dimensions, although the extension of the present paper to two dimensions is not seen as a significant complexity.

However, each cycle of his proposed iteration requires full solution of the equation corresponding to Equation (3), without exploiting the particular nature of the binary nonlinearity, so the solution is relatively slow.

To reduce the solution time for this procedure, Vollebregt, Kalker and Lin [14] give some details of an indirect method based on Gauss-Seidel iteration. This gives advantage when the same influence function is used throughout the elastic system (the columns and rows of $[W]$ are identical but shifted) in which case the process converges in $O(n^2)$ operations as opposed to $O(n^3)$ for direct solution. The authors admit to some convergence difficulties in this paper, which are addressed by Vollenbregt [15]. Such a method clearly has application to the model of the present paper in cases where a single influence function may be used, and would allow reduced matrix storage and potentially improved solution speed.

A more advanced approach to indirect solution is given by Venner and Lubrecht [16] who use a multilevel solution to reduce the complexity of the iterative process, while increasing its convergence rate. They take advantage of the localised effect of each discrete force element in a concentrated contact problem to develop an improved relaxation method, and then improve this by refining the solution between coarse and fine grids. In an ideal situation with known contact region this would lead to a solution in $O(n^{-d}\log n^{-d})$ operations, where d is the dimension of the problem. However the free boundary of the contact constraint complicates the solution as loss of contact at some point in the model causes a disturbance to the entire solution, not just in the region of the point in question, and they comment that this causes degraded convergence.

The utility of these different approaches will vary with the requirements of specific applications. Indirect methods have the attraction of finding an approximate solution early in the process, but may have convergence problems. Direct methods clearly achieve exact solutions, but may be slower and require more storage. If the initial estimate of contact region $\boldsymbol{\beta}$ is reasonably accurate, the method of this paper gives a solution in $O(n^2)$ operations which is similar to that of Vollebregt. Venner and Lubrecht's claim to efficiency of $O(n^{-d}\log n^{-d})$ is ambitious given their difficulty in identifying the free boundary. The simplification allowed by both Vollebregt *et al*., and Venner and Lubrect that the same influence function be used throughout the model could be applied to the work of this paper to advantage. The limited extent of a Flamant influence function gives a banded weighting function matrix $[W]$ which could be exploited also. Furthermore, this paper offers a solution which maintains a close relation to the physical problem being solved. Kalker [13, p51] draws an important contrast between "mathematical programming solutions which can be established rigorously, but have the drawback that they are not easy to interpret mechanically" and "*Ad hoc* methods that have the advantage that the engineer can understand what is happening, but the drawback that they cannot be proved to converge." The method given here aims to be an appropriate tool for solution of practical problems.

The work has been presented as a solution for frictionless elastic contact problems, but will apply elsewhere when similar binary nonlinearities exist. Work on surface roughness may benefit, as the decision as to when a local peak of the surface yields could be treated as a binary nonlinearity with the same method used to switch between elastic and plastic stresses. Poon and Sayles [17] address this problem and require two nested iterative loops to deal with contact uncertainty and elastic-plastic transition. As they assume non-work hardening behaviour, their model could be treated either as two sets of binary nonlinearities, or the work of this paper could be extended to "ternary nonlinearities" to allow only compressive stress between the bodies, restricted to an upper limit. This approach would be identical to

that required to describe stick-slip friction and would allow faster modelling of fretting and other friction-dependent problems. The work may also have application in the imposition of non-negative constraints in mathematical programming problems.

9. Conclusion

This paper has addressed the binary nonlinearity in modelling mechanical contact of two approaching elastic bodies which arises due to uncertainty over the extent of their mutually contacting interface. The work applies to any discrete model of elastic behaviour and is not limited to a specific deformation function or geometry. The problem has been expressed in partitioned matrix form, which can be solved by partial Gauss-Jordan elimination. The elimination process is governed by the search for an equilibriate non-negative solution and leads to rapid answers. The stability of the iterative approach has been proven and worked examples given. The technique is general and can be applied to other fields where binary nonlinearities occur.

References

1. H. Hertz, Über die Berührung fester elastischer Körper. *J. reine und angewandte Mathematik* 92 (1882) 156–171.
2. K.L. Johnson, *Contact Mechanics*. Cambridge: Cambridge University Press (1985) 452pp.
3. D.A. Hills, D. Nowell and A. Sackfield, *Mechanics of Elastic Contacts.* New York: McGraw Hill (1993) 496pp.
4. S.P. Timoshenko and J.N. Goodier, *Theory of Elasticity*. 2nd. edn. Oxford: Butterworth-Heinemann Ltd (1993) 506pp.
5. Y.P. Chiu, A.S. Weinstein and C.F. Zorowski, The stresses, deformations and bending of a simply supported cylinder subjected to a symmetric normal surface loading. *Int. J. Mech. Sci.* 5 (1963) 119–136.
6. G.P. Steven, A non-axisymmetric cylindrical contact problem. *Int. J. Engng. Sci.* 15 (1977) 95–103.
7. Y.P. Chiu and M.J. Hartnett, A numerical solution for the contact problem involving bodies with cylindrical surface considering cylinder effect. *J. Tribology* 109 (1987) 479–485.
8. N. Ahmadi, L.M. Keer and T. Mura, Non-Hertzian contact stress analysis for an elastic half space-normal and sliding contact. *Int. J. Solids Structures* 19 (1983) 357–373.
9. J.J. Kalker and Y. van Randen, A minimum principle for frictionless elastic contact with application to non-Hertzian half-space contact problems. *J. Eng. Maths.* 6 (1972) 193–206.
10. J.M. Allwood, *Online Modelling and Control of Shape Phenomena in Metal Rolling*. U. of London: PhD thesis (1994) 210pp.
11. F.R. Gantmacher, *The Theory of Matrices*. New York: Chelsea (1959) 374pp.
12. W.W. Hager, Updating the inverse of a matrix. *SIAM Review* 31 (1989) 221–239.
13. J.J. Kalker, *Three-dimensional Elastic Bodies in Rolling Contact.* Dordrecht: Kluwer Academic Publishers (1990) 314pp.
14. E.A.H. Volbrecht, J.J. Kalker and H.X. Lin, A fast solver for normal and tangential contact mechanics in the half-space. In: *Contact Mechanics (Computational Techniques)* Eds. M.H. Aliabadi, C.A. Brebbia; Southampton: Computational Mechanics Publications (1993) 235–242.
15. E.A.H. Volbregt, A Gauss-Seidel type solver for special convex programs, with application to frictional contact mechanics. *J. Opt. Th. and Appl.* 87 (1995) 47–67.
16. C.H. Venner and A.A. Lubrecht, Multilevel solution and integro-differential equations in contact mechanics and lubrication. *Proc EMG 93*, Birkhauser Verlag (1994) 111–128.
17. C.Y. Poon and R.S. Sayles, Numerical contact model of a smooth ball on an anisotropic rough surface. *Trans. ASME* 116 (1994) 194–201.